MITSUBISHI ELECTRIC RESEARCH LABORATORIES
https://www.merl.com

Overhead Reduction for Graph-Based Point Cloud Delivery Using Non-Uniform Quantization

Fujihashi, Takuya; Koike-Akino, Toshiaki; Watanabe, Takashi

TR2022-005 January 15, 2022

Abstract

Graph-based compression can compact the signal energy of the three-dimensional (3D) point cloud and realize high- quality 3D point cloud delivery over wireless channels. However, it requires significant communication overhead of graph Fourier transform (GFT) orthogonal matrix. For significant overhead reduction, our scheme integrates two methods: Givens rotation and non-uniform quantization. The Givens rotation transforms the GFT orthogonal matrix into angle parameters. The angle parameters are then non-uniformly quantized based on an empir- ical concave cumulative distribution function (CDF). Evaluation results show the proposed scheme reduces 28.6% communication overhead and improve up to 3.8dB 3D reconstruction quality compared with the conventional schemes.

IEEE International Conference on Consumer Electronics (ICCE) 2022

Mitsubishi Electric Research Laboratories, Inc.
201 Broadway, Cambridge, Massachusetts 02139

Overhead Reduction for Graph-Based Point Cloud Delivery Using Non-Uniform Quantization

Soushi Ueno*, Takuya Fujihashi*, Toshiaki Koike-Akino†, Takashi Watanabe*
*Graduate School of Information and Science, Osaka University, Osaka, Japan
†Mitsubishi Electric Research Laboratories (MERL), Cambridge, MA 02139, USA

***Abstract*—Graph-based compression can realize a high-quality delivery of three-dimensional (3D) point cloud data over wireless channels. However, it requires a significant amount of communication overhead in sending a graph Fourier transform (GFT) orthogonal matrix. To reduce the overhead, we integrate two methods: Givens rotation and non-uniform quantization. The Givens rotation transforms the GFT orthogonal matrix into angle parameters, and then they are non-uniformly quantized to maintain high quality at low overheads. We demonstrate that the proposed scheme can reduce a communication overhead by 28.6% and improve a 3D reconstruction quality by up to 3.8 dB compared with the conventional schemes.**

I. Introduction

Recent advances in wide-band wireless technologies have fueled a wide range of emerging applications. In particular, volumetric video streaming plays an important role as one of enabling technologies for mixed reality (XR) and will become a key application of advanced wireless networks, as shown in Fig. 1. In fact, some contents providers, including Google and Meta, have started to develop volumetric video streaming for consumer services. Point cloud [1] is arguably the most popular volumetric data structure for three-dimensional (3D) contents [2]. It represents the 3D scene using a numerous number of 3D points. Each point has attributes of 3D coordinates and color components and is not uniformly distributed over 3D space in general.

The point cloud streaming over wireless channels has two major challenges. The first challenge is how to efficiently compress and send such a numerous and irregular structure of the 3D points within a limited bandwidth allocation. Uncompressed point cloud data will cause a large traffic for streaming over wireless networks. Specifically, each 3D point typically takes 15 bytes: 4 bytes for each 3D coordinate and 1 byte for each color component. For example, streaming a point cloud frame with 200K 3D points requires $15 \times 200{,}000 = 3$ Mbytes, and thus approximately 720 Mbps at a frame rate of 30 fps.

Several digital-based solutions, such as Draco [3] and point cloud library (PCL) [4], [5], have been proposed for point cloud compression and decompression. Draco employs k-d tree [6] based compression while PCL is based on Octree [7]. These algorithms generate a compressed bitstream for the 3D coordinates and color components. However, such solutions have limited coding efficiency in general since they remain redundant information between the 3D points. To fully utilize the correlations between the 3D points for compression, graph signal processing (GSP) [8] was introduced for point cloud

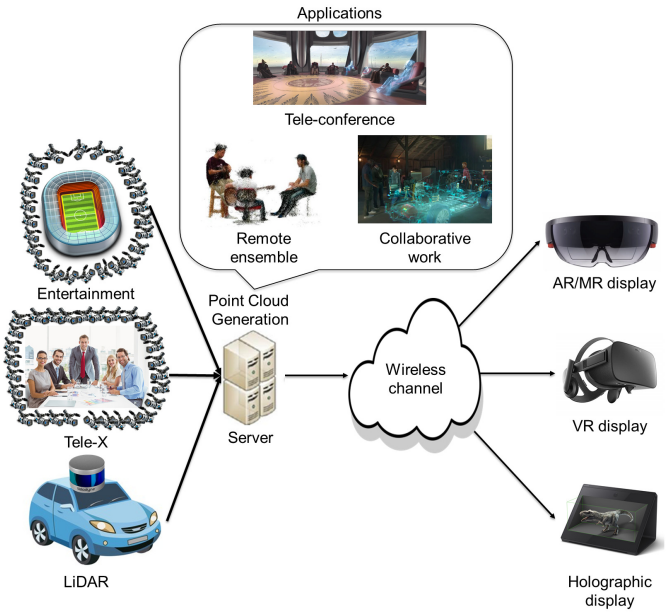

Fig. 1. Applications for wireless point cloud delivery.

delivery. Specifically, the 3D points are regarded as a weighted and undirected graph, and then graph Fourier transform (GFT) [9] is carried out for decorrelation of the graph signals. The GFT efficiently compacts the signal energy compared with the conventional transformation techniques, e.g., discrete Fourier transform (DFT) and discrete cosine transform (DCT), used for 2D images. On the other hand, the GFT-based coding needs to accommodate a large communication overhead for signal decoding.

The second challenge is the resilience to the quality fluctuation of wireless channels. The transmission part of the point cloud streaming sequentially uses channel coding and digital modulation schemes to send the compressed bitstream to a wireless holographic display. However, the existing solutions suffer from the following problems due to the wireless channel unreliability. First, the encoded bitstream is highly vulnerable to bit errors [10] occurred in wireless channels. Below a certain signal-to-noise ratio (SNR), wireless fading can cause catastrophic errors for entropy decoding of point cloud data, resulting in significant degradation of 3D reconstruction quality. This phenomenon is called cliff effect [11]. Second,

the reconstruction quality does not improve even when the wireless channel quality is improved unless an adaptive rate control of source and channel coding is performed in a real-time manner according to the rapid fading channels. This is called leveling effect.

To tackle the above-mentioned challenges, we propose a novel scheme for wireless point cloud delivery inspired by HoloCast [12]. The key ideas of the proposed scheme are three-fold: 1) taking GFT for each attribute in graph signals to compact the signal power whose output is then scaled and directly mapped to transmission signals using analog modulation [13]; 2) skipping nonlinear operations, e.g., quantization and entropy coding, for GFT coefficients to prevent the cliff effect; and 3) integrating Givens rotation and non-uniform quantization for GFT orthogonal matrix for a low communication overhead. We demonstrate that the proposed scheme simultaneously solves cliff and leveling effects even in unstable wireless channels and achieves a communication overhead reduction by up to 28.6% using the proposed non-uniform quantization.

Related Works and Contributions: Some related soft delivery schemes have been proposed for wireless video delivery, including immersive video contents. For example, FreeCast [14] is designed for 5D ordered multi-view video plus depth (MVD) signals, while the studies in [15], [16] designed soft delivery schemes for 360-degree videos. Instead of quantization and entropy coding, those soft delivery schemes use a unitary transform and analog modulation, which maps the coefficients directly to transmission signals, to realize a reconstructed quality proportional to wireless channel quality. HoloCast [12] designed a GFT-based soft delivery for the 3D point cloud. HoloCast can deal with the non-ordered and non-uniformly distributed points in coding and decoding.

The main purpose of our study is to reduce the communication overhead required to send the GFT orthogonal matrix in HoloCast. The proposed scheme has the following major contributions:

- We introduce the Givens rotation [17], [18] for the GFT orthogonal matrix to represent any unitary orthogonal matrices with a small number of angle parameters.
- We investigate the distribution of the angle parameters for efficient quantizations.
- We integrate non-uniform quantization parameterized by a single controllable value into the Givens rotation.

Although the Givens rotation is mainly studied with uniform quantization [17]–[19], the distribution mismatch of the angle parameters causes inefficient compression of the parameters. We found that the angle parameters are non-uniformly distributed, and hence the non-uniform quantization can efficiently reduce the amount of communication overhead to send the angle parameters as metadata for reconstruction.

II. Graph Signal Processing for Point Cloud

We first describe some basics of graph signal processing for the 3D point cloud.

A. Graph Construction

The 3D point cloud consists of the 3D coordinates and color components. Both 3D coordinates and color components can be regarded as a weighted and undirected graph $\boldsymbol{G} = (\boldsymbol{V}, \boldsymbol{E}, \boldsymbol{W})$. Here, $\boldsymbol{V}$ is the vertex set and $\boldsymbol{E}$ is the edge set. $\boldsymbol{W}$ is an adjacency matrix to represent each edge weight. Specifically, $\boldsymbol{W}_{i,j}$ represents the edge weight between vertices i and j. The 3D coordinates $\boldsymbol{p} = [\mathrm{x}, \mathrm{y}, \mathrm{z}]^{\mathrm{T}} \in \mathbb{R}^{3\times N}$ and the corresponding color components $\boldsymbol{c} = [y, u, v]^{\mathrm{T}} \in \mathbb{R}^{3\times N}$ can be regarded as graph signals that reside on the vertices. Here, N is the number of vertices in the point cloud.

B. Graph Fourier Transform (GFT)

We consider each edge weight $\boldsymbol{W}_{i,j}$ of the graph signals can be obtained as follows [20]:

$$\boldsymbol{W}_{i,j} = \exp\left(-\left(\frac{\|\boldsymbol{p}_i - \boldsymbol{p}_j\|_2^2}{\epsilon_p} + \frac{\|\boldsymbol{c}_i - \boldsymbol{c}_j\|_2^2}{\epsilon_c}\right)\right), \quad (1)$$

where ϵ_p and ϵ_c are the sample variance of 3D coordinates and color components, respectively. The graph signals are then transformed into frequency-domain coefficients using GFT. The GFT is defined through the graph Laplacian operator $\boldsymbol{L} \in \mathbb{R}^{N\times N}$ based on the adjacency matrix $\boldsymbol{W} \in \mathbb{R}^{N\times N}$ as follows:

$$\boldsymbol{L} = \boldsymbol{D} - \boldsymbol{W}, \quad (2)$$

where $\boldsymbol{D} \in \mathbb{R}^{N\times N}$ is the diagonal degree matrix:

$$\boldsymbol{D} = \mathrm{diag}(D_1, D_2, \ldots, D_N), \qquad D_i = \sum_{n=1}^{N} \boldsymbol{W}_{i,n}. \quad (3)$$

In general, the graph Laplacian is a real symmetric matrix that has a complete set of orthonormal eigenvectors with corresponding nonnegative eigenvalues. The eigenvectors and eigenvalues of the graph Laplacian operator can be obtained by the eigenvalue decomposition as:

$$\boldsymbol{L} = \boldsymbol{\Phi}\boldsymbol{\Lambda}\boldsymbol{\Phi}^{-1}, \quad (4)$$

where $\boldsymbol{\Lambda} \in \mathbb{R}^{N\times N}$ is a diagonal matrix of the eigenvalues and $\boldsymbol{\Phi} \in \mathbb{R}^{N\times N}$ is a matrix of the eigenvectors, i.e., GFT orthogonal matrix. The GFT frequency-domain coefficients $\boldsymbol{s} \in \mathbb{R}^{3\times N}$ are obtained by multiplying the GFT orthogonal matrix by the attribute signals $\boldsymbol{f} \in \mathbb{R}^{3\times N}$ as

$$\boldsymbol{s} = \boldsymbol{f}\,\boldsymbol{\Phi}, \quad (5)$$

where $\boldsymbol{f}$ is either 3D coordinates matrix $\boldsymbol{p}$ or color attributes matrix $\boldsymbol{c}$. Note that each attribute can be reconstructed from GFT coefficients using the GFT orthogonal matrix as $\boldsymbol{f} = \boldsymbol{s}\,\boldsymbol{\Phi}^{-1}$. This is called inverse GFT (IGFT).

III. Proposed Soft Point Cloud Delivery

A. Overview of Sender and Receiver Operations

The objectives of the proposed scheme are 1) to prevent cliff and leveling effects owing to wireless channel quality fluctuation and 2) to reduce communication overhead with high quality. Fig. 2 shows an overview of the proposed

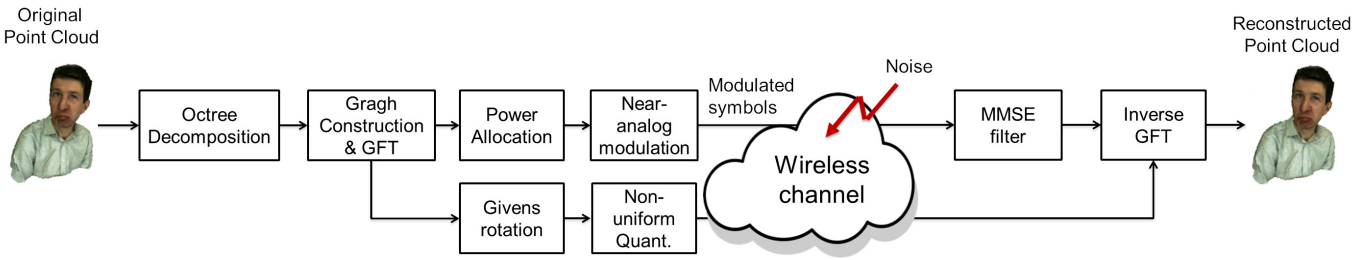

Fig. 2. Overview of the proposed scheme using non-uniform quantization for the compression of GFT orthogonal matrix.

scheme. The graph signals corresponding to the 3D point cloud are firstly split into independent blocks using octree decomposition. For the attributes in each block, the sender employs GFT for decorrelation and assigns transmission power to each GFT coefficient in accordance with HoloCast [12]. The GFT coefficients are modulated to a dense constellation, i.e., pseudo-analog modulation [13], for transmission. In addition, the Givens rotation is introduced to the GFT orthogonal matrix to represent it with angle parameters. For the quantization of the angle parameters, we optimize non-uniform quantization intervals. The receiver carries out IGFT followed by a minimum mean-square error (MMSE) filter for the received GFT coefficients to reconstruct 3D coordinates and color components. Here, the GFT orthogonal matrix can be reconstructed from the received angle parameters.

B. Givens Rotation for GFT Orthogonal Matrix

In the conventional graph-based point cloud delivery schemes, the receiver needs to know the eigenvectors matrix, i.e., $\boldsymbol{\Phi}$, for reconstructing 3D coordinates and color components. Hence, the sender transmits N^2 real elements to the receiver as metadata in each octree block when N is the number of 3D points in an octree block.

The GFT orthogonal matrix is unitary so that the orthogonal matrix can be decomposed into a product of at most $N(N-1)/2$ Givens rotations according to [18]. We reduce the number of metadata transmissions via the Givens rotation. In general, there exist many possible factorizations. We start with the GFT orthogonal matrix $\boldsymbol{\Phi}$ and introduce zeros to columns from left to right without diagonal elements. In the proposed scheme, the eigenvectors matrix $\boldsymbol{\Phi} \in \mathbb{R}^{N\times N}$ is decomposed as follows:

$$\boldsymbol{\Phi} = \prod_{k=1}^{N} \Big[\boldsymbol{D}_k(\phi_{k,k}, \ldots, \phi_{k,N}) \prod_{l=k+1}^{N} \boldsymbol{G}_{k,l}(\psi_{k,l}) \Big], \quad (6)$$

$$\boldsymbol{D}_k(\phi_{k,k}, \ldots, \phi_{k,N}) = \mathrm{diag}(\mathbf{1}_{k-1}, \mathrm{e}^{\jmath\phi_{k,k}}, \ldots, \mathrm{e}^{\jmath\phi_{k,N}}),$$

where $\mathbf{1}_{k-1}$ is an all-ones vector of size $k-1$, and $\boldsymbol{G}_{k,l}(\psi)$ is Givens rotation matrix in rows k and l as follows:

$$\boldsymbol{G}_{k,l}(\psi) = \begin{bmatrix} \boldsymbol{I}_{k-1} & & & & \\ & c & & -s & \\ & & \boldsymbol{I}_{l-k-1} & & \\ & s & & c & \\ & & & & \boldsymbol{I}_{N-l} \end{bmatrix},$$

where $\boldsymbol{I}_k$ is $k \times k$ identity matrix, $c = \cos(\psi)$ and $s = \sin(\psi)$. Hence any orthogonal matrix is represented with angle variables of $\phi_{k,l}$ $(1 \le k \le N, k \le l \le N)$ and $\psi_{k,l}$ $(1 \le k \le N-1, k+1 \le l \le N)$.

We explain the parameterization procedure with a 3×3 eigenvectors matrix $\boldsymbol{\Phi}$ as follows:

$$\boldsymbol{\Phi} = \begin{bmatrix} \times & \times & \times \\ \times & \times & \times \\ \times & \times & \times \end{bmatrix} \xrightarrow{\boldsymbol{D}_1^T} \begin{bmatrix} |\times| & \times & \times \\ |\times| & \times & \times \\ |\times| & \times & \times \end{bmatrix} \xrightarrow{\boldsymbol{G}_{1,2}^T, \boldsymbol{G}_{1,3}^T} \begin{bmatrix} 1 & 0 & 0 \\ 0 & \times & \times \\ 0 & \times & \times \end{bmatrix}$$
$$\xrightarrow{\boldsymbol{D}_2^T} \begin{bmatrix} 1 & 0 & 0 \\ 0 & |\times| & \times \\ 0 & |\times| & \times \end{bmatrix} \xrightarrow{\boldsymbol{G}_{2,3}^T} \begin{bmatrix} 1 & 0 & 0 \\ 0 & 1 & 0 \\ 0 & 0 & \times \end{bmatrix} \xrightarrow{\boldsymbol{D}_3^T} \begin{bmatrix} 1 & 0 & 0 \\ 0 & 1 & 0 \\ 0 & 0 & 1 \end{bmatrix} = \boldsymbol{I}_3,$$

where $|\cdot|$ is the absolute value of the corresponding element. At the first step, the proposed scheme makes all the entries in the first column under the first component all zeros. To do so, we extract the angle information from the first column by multiplying $\boldsymbol{\Phi}$ by $\boldsymbol{D}_1^T$ to have a positive-valued column, and then applying a series of Givens matrices with appropriate parameters to make all entries under $(1,1)$ element zeros. Since the Givens rotation keeps the length of the vector, the $(1,1)$ element will be 1. At the same time, all the entries in the first row except the $(1,1)$ element also become zeros because of the orthogonality between the columns. We carry similar procedures on the remaining columns sequentially, and finally, we have an identity matrix $\boldsymbol{I}_N$. Since each Givens matrix is a unitary matrix, the matrix $\boldsymbol{\Phi}$ can be factorized as:

$$\boldsymbol{\Phi} = \boldsymbol{D}_1(\phi_{1,1}, \ldots, \phi_{1,3}) \boldsymbol{G}_{1,2}(\psi_{1,2}) \boldsymbol{G}_{1,3}(\psi_{1,3}) \cdot \boldsymbol{D}_2(\phi_{2,2}, \ldots, \phi_{2,3}) \boldsymbol{G}_2(\psi_{2,3}) \boldsymbol{D}_3(\phi_{3,3}).$$

When we have an original parameter set, i.e., the rotation angles $\{\phi_{k,l}, \psi_{k,l}\}$, we can exactly reconstructs the original matrix $\boldsymbol{\Phi}$. However, the transmission of the angle parameters still causes a large communication overhead. Therefore, the proposed scheme quantizes the angle parameters set ϕ and ψ before transmission. Since the GFT orthogonal matrix consists of the real elements, the angle ϕ is 0 or π and thus the binary quantization suffices.

C. Non-Uniform Quantization

In the standard Givens-based compression [18], the rotation angles ψ are uniformly quantized between 0 and $\pi/2$ as given

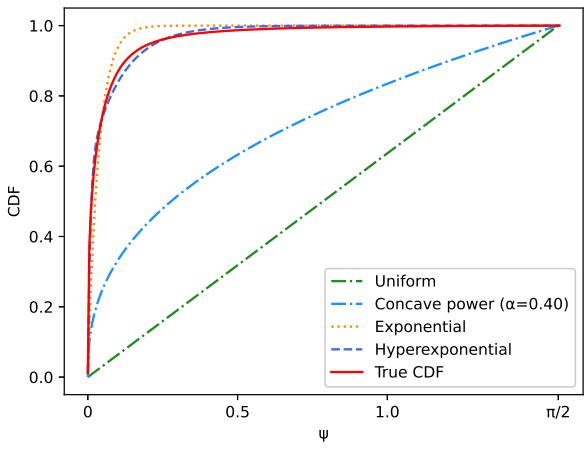

Fig. 3. The cumulative distribution of the angle parameters in graph Laplacian for the 3D point cloud of *pencil_10_0*, whose number of points is 2,731.

by the following equation:

$$\psi = \frac{\pi}{2} \cdot \frac{2n+1}{2^{b+1}}, \qquad n = 0, 1, \ldots, 2^b - 1, \tag{7}$$

where b is the number of bits used for the quantization of ψ. Specifically, the quantization in (7) assumes the angle parameters of ψ follow the uniform distribution.

However, we empirically found that the angle parameters for the graph Laplacian follow the non-uniform distribution. Fig. 3 shows the empirical cumulative distribution function (CDF) of the angle parameters ψ for a reference 3D point cloud data of *pencil_10_0*, whose number of points is 2,731. We can see that most of the angle parameters are close to zero. It suggests that we can more efficiently quantize the angle parameters by exploiting the non-uniformity. It was shown that hyper-exponential and exponential distributions agree well with the empirical CDF. We note the hyper-exponential CDF can be given by the following equation:

$$F_{\text{h.exp}}(\psi) = (1-\rho)(1 - \beta_1 e^{-\gamma_1 \psi} - \beta_2 e^{-\gamma_2 \psi}) + \rho, \tag{8}$$

where ρ is the ratio of zero-value of ψ and β_l and γ_l are fitting parameters. Here, we present the CDF curves with the best fitting parameters of β and γ under a condition of $\beta_1 + \beta_2 = 1$.

Besides the hyper-exponential function, we introduce a concave CDF based on power function:

$$F(\psi) = \left(\frac{2}{\pi}\psi\right)^{\alpha}, \tag{9}$$

where $\alpha < 1$ is an adjustable parameter. Based on the concave CDF, each angle parameter ψ is quantized between 0 and $\pi/2$ as given by the following equation:

$$\psi \simeq \frac{1}{2}(x_n + x_{n+1}), \qquad n = 0, 1, \ldots, 2^b - 1, \tag{10}$$

$$x_{n'} = F^{-1}\left(\frac{n'}{2^b}\right) = \frac{\pi}{2}\left(\frac{n'}{2^b}\right)^{1/\alpha}, \qquad n' = 0, 1, \ldots, 2^b,$$

where $F^{-1}(\cdot)$ is an inverse concave CDF. This concave CDF with a small value of α can decrease the gap from the true distribution compared with the uniform distribution. Although the hyper-exponential distribution matches the true distribution more closely as shown in Fig. 3, we will show that an error propagation in the Givens rotations causes quality degradation if we use too strong non-uniformity. We discuss the effect of the assumed distribution on 3D reconstruction quality later.

IV. Experiments

A. Settings

*1) **Metric**:* We define the reconstruction quality of point cloud in terms of the symmetric MSE based on [21] in the attribute of color components $\boldsymbol{c}$.

*2) **Point Cloud Dataset**:* We use the reference point cloud, namely, *pencil__10_0* and *milk_color*, whose number of points is 2,731 and 13,704, respectively. We first use *pencil__10_0* to clarify the baseline performance. For the discussion on visual quality, we use *milk_color*. Since the number of points is large, the 3D points are split into blocks using the octree decomposition. Here, each block can contain up to 5,000 3D points.

*3) **Wireless Configuration**:* The analog-modulated GFT coefficients are impaired by an additive white Gaussian noise (AWGN) channel. Specifically, an effective noise follows the complex Gaussian distribution $\mathcal{CN}(0, \sigma^2)$ with a variance of σ^2.

B. Overhead Reduction

We first evaluate the 3D reconstruction quality in the conventional HoloCast [19] and the proposed scheme as a function of the number of bits for each angle ψ. For discussion on the assumed distribution for non-uniform quantization, we prepare another comparative HoloCast using hyper exponential-based non-uniform quantization, which agrees well with the empirical CDF. Fig. 4 shows the symmetric MSE as a function of the number of bits for each angle parameter at a wireless channel SNR of 25 dB. Here, we set the parameter of α for the proposed non-uniform quantization to 0.4. We later discuss the optimal parameter of α in Sec. IV-D. We find the following key observations:

- The 3D reconstruction quality can be improved with an increase of the number of bits b in our scheme.
- HoloCast with hyper exponential-based non-uniform quantization does not improve the reconstruction quality even when the number of bits increases. It may be because a large quantization error occurs at larger angles.
- Even at a lower number of bits, the proposed scheme yields better quality.

For example, the proposed scheme achieves an overhead reduction by up to 28.6% and an MSE reduction by up to 3.8 dB compared with the conventional HoloCast using uniform quantization.

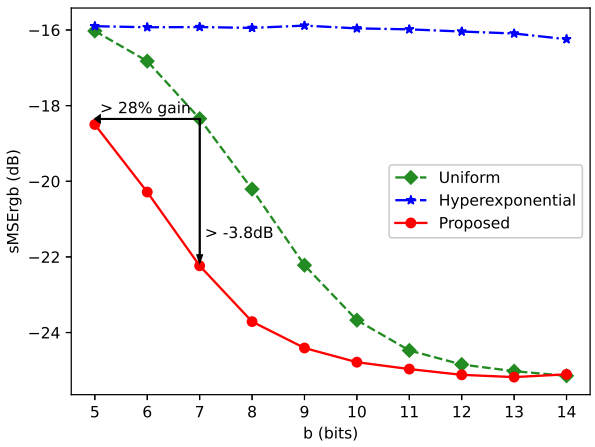

Fig. 4. MSE of color attributes as a function of the number of bits for each angle parameter. Here, wireless channel SNR is 25 dB.

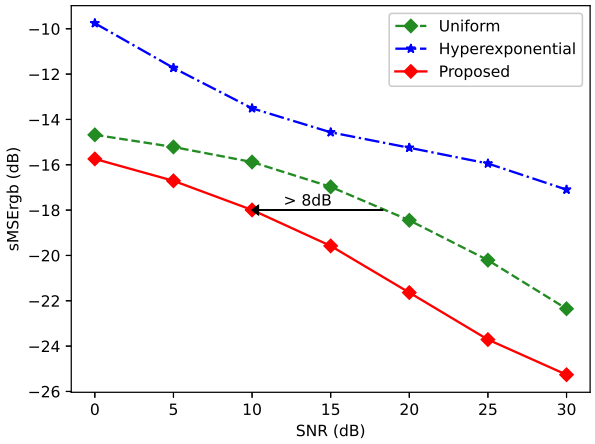

Fig. 5. MSE of color attributes as a function of wireless channel SNR at a quantization bit of $b = 8$.

C. Quality vs. Channel SNR

Here, we discuss the effect of the wireless channel quality on the 3D reconstruction quality. Fig. 5 shows the symmetric MSE as a function channel SNR for $b = 8$. The proposed scheme can reconstruct a clean 3D point cloud compared with the other schemes under the same communication overhead irrespective of wireless channel SNRs. For example, the improvement of color reconstruction quality from the uniform quantization and hyper-exponential quantization is 2.41 dB and 6.11 dB on average, respectively, across the wireless channel SNRs from 0 dB to 30 dB. Accordingly, the proposed method achieves a significant SNR gain greater than 8 dB over the uniform quantization.

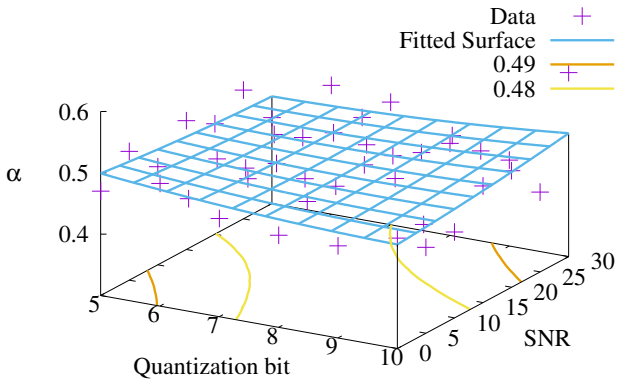

Fig. 6. The optimal value of α as a function of wireless channel SNR and the number of bits for each angle parameter.

D. Discussion on Non-Uniform Quantization

This section discusses the best value of the non-uniform quantization parameter α according to the quality of the wireless channel and the quantization level. Fig. 6 shows the optimal values of α. To obtain the optimal values, we evaluated the 3D reconstruction quality by sweeping α with 0.01 interval in a finite grid under a different quantization level and channel SNR. From the result, the optimized α can be modeled by a quadratic function of $f(b,q) = a_0b^2 + a_1q^2 + a_2bq + a_3b + a_4q + a_5$, where b and q are quantization level in bits and SNR in dB, respectively. More specifically, the optimal parameters can be derived by using least-squares fitting as follows:

$$\alpha_{\text{opt}} \simeq 9.1 \cdot 10^{-4} \cdot b^2 + 1.4 \cdot 10^{-5} \cdot q^2 + 3.7 \cdot 10^{-4} \cdot bq + 5.7 \cdot 10^{-1} \cdot b - 1.9 \cdot 10^{-2} \cdot q - 3.1 \cdot 10^{-3}. \quad (11)$$

From the fitting result, we can see that the optimal value of α is between 0.4 and 0.6 in any b and q. The quality gap is up to 0.4 dB over this range of α.

E. Visual Quality

Finally, we discuss the visual quality to further make clear the effect of the non-uniform quantization. Figs. 7 (a)–(f) present the visual quality at a wireless channel SNR of 20 dB for different quantization bits b. The visual quality of the conventional HoloCast with Givens rotation and uniform quantization is low under the limited amount of overhead. In contrast, higher visual quality can be achieved in the proposed scheme under the same amount of communication overhead.

V. Conclusion

In this paper, we proposed a novel scheme realizing a high-quality point cloud delivery under a low communication overhead. The proposed scheme integrates the Givens rotation and non-uniform quantization for the compression of the GFT orthogonal matrix. Specifically, the Given rotation transforms

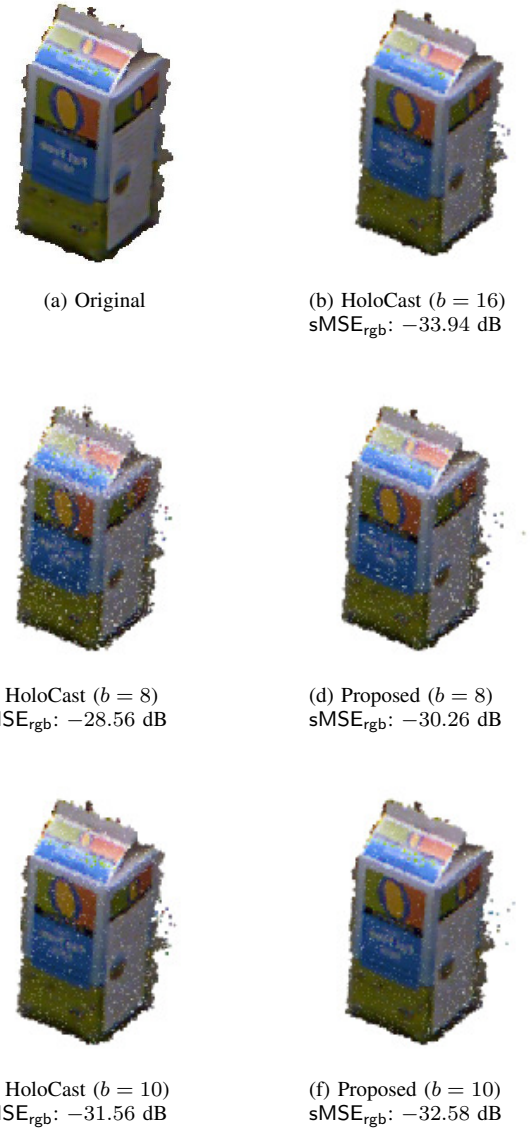

(a) Original

(b) HoloCast ($b = 16$) $\mathsf{sMSE}_{\mathsf{rgb}}$: -33.94 dB

(c) HoloCast ($b = 8$) $\mathsf{sMSE}_{\mathsf{rgb}}$: -28.56 dB

(d) Proposed ($b = 8$) $\mathsf{sMSE}_{\mathsf{rgb}}$: -30.26 dB

(e) HoloCast ($b = 10$) $\mathsf{sMSE}_{\mathsf{rgb}}$: -31.56 dB

(f) Proposed ($b = 10$) $\mathsf{sMSE}_{\mathsf{rgb}}$: -32.58 dB

Fig. 7. Snapshots at wireless channel SNR of 20 dB for different b values.

the GFT orthogonal matrix into angle parameters and the non-uniform quantization compresses the angle parameters. We showed that the non-uniform quantization in the proposed scheme yields both better reconstruction quality and lower communication overhead compared with the uniform quantization. It was demonstrated that a significant SNR gain greater than 8 dB is attainable.

ACKNOWLEDGMENT

T. Fujihashi's work was partly supported by JSPS KAKENHI Grant Number 17K12672.

REFERENCES

[1] R. Mekuria and L. Bivolarsky, "Overview of the MPEG activity on point cloud compression," in *Data Compression Conference*, 2016, p. 620.

[2] P. Su, W. Cao, J. Ma, B. Cheng, X. Liang, L. Cao, and G. Jin, "Fast computer-generated hologram generation method for three-dimensional point cloud model," *Journal of Display Technology*, vol. 12, no. 12, pp. 1688–1694, 2016.

[3] "Draco 3D data compression." [Online]. Available: https://google.github.io/draco/

[4] J. Kammerl, N. Blodow, R. B. Rusu, S. Gedikli, M. Beetz, and E. Steinbach, "Real-time compression of point cloud streams," in *IEEE International Conference on Robotics and Automation*, 2012, pp. 778–785.

[5] K. Muller, H. Schwarz, D. Marpe, C. Bartnik, S. Bosse, H. Brust, T. Hinz, H. Lakshman, P. Merkle, F. H. Rhee, G. Tech, M. Winken, and T. Wiegand, "3D is here: Point cloud library (PCL)," in *IEEE International Conference on Robotics and Automation*, 2011, pp. 1–4.

[6] O. Devillers and P. Gandoin, "Geometric compression for interactive transmission," in *Visualization*, 2000, pp. 319–326.

[7] R. schnabel and R. Klein, "Octree-based point-cloud compression," in *Eurographics Symposium on Point-Based Graphics*, 2006, pp. 111–121.

[8] A. Ortega, P. Frossard, J. Kovacevic, J. M. F. Moura, and P. Vandergheynst, "Graph signal processing: Overview, challenges, and applications," *Proceedings of the IEEE*, vol. 106, no. 5, pp. 808–828, 2018.

[9] C. Zhang, D. Florêncio, and C. Loop, "Point cloud attribute compression with graph transform," in *2014 IEEE International Conference on Image Processing (ICIP)*, 2014, pp. 2066–2070.

[10] S. Pudlewski, N. Cen, Z. Guan, and T. Melodia, "Video transmission over lossy wireless networks: A cross-layer perspective," *IEEE Journal of Selected Topics in Signal Processing*, vol. 9, no. 1, pp. 6–21, 2015.

[11] T. Fujihashi, T. Koike-Akino, T. Watanabe, and P. V. Orlik, "High-quality soft video delivery with GMRF-based overhead reduction," *IEEE Transactions on Multimedia*, vol. 20, no. 2, pp. 473–483, Feb. 2018.

[12] T. Fujihashi, T. Koike-Akino, T. Watanabe, and P. Orlik, "HoloCast: Graph signal processing for graceful point cloud delivery," in *IEEE International Conference on Communications*, 2019, pp. 1–7.

[13] S. Jakubczak and D. Katabi, "A cross-layer design for scalable mobile video," in *ACM Annual International Conference on Mobile Computing and Networking*, Las Vegas, NV, sep 2011, pp. 289–300.

[14] T. Fujihashi, T. Koike-Akino, T. Watanabe, and P. V. Orlik, "FreeCast: Graceful free-viewpoint video delivery," *IEEE Transactions on Multimedia*, vol. PP, no. 99, pp. 1–11, 2019.

[15] J. Zhao, R. Xiong, and J. Xu, "OmniCast: Wireless pseudo-analog transmission for omnidirectional video," *IEEE Journal on Emerging and Selected Topics in Circuits and Systems*, vol. 9, no. 1, pp. 58–70, 02 2019.

[16] Y. Lu, T. Fujihashi, S. Saruwatari, and T. Watanabe, "360cast+: Viewport adaptive soft delivery for 360-degree videos," *IEEE Access*, vol. PP, no. 99, pp. 1–14, 2021.

[17] M. A. Sadrabadi, A. Khandani, and F. Lahouti, "Channel feedback quantization for high data rate MIMO systems," *IEEE Transactions on Wireless Communications*, vol. 5, no. 12, pp. 3335–3338, 2006.

[18] J. C. Roh and B. D. Rao, "Efficient feedback methods for MIMO channels based on parameterization," *IEEE Transactions on Wireless Communications*, vol. 6, no. 1, pp. 282–292, 2007.

[19] T. Fujihashi, T. Koike-Akino, T. Watanabe, and P. Orlik, "Overhead reduction in graph-based point cloud delivery," in *IEEE International Conference on Communications*, 2020, pp. 1–7.

[20] X. Liu, G. Cheung, X. Wu, and D. Zhao, "Random walk graph Laplacian based smoothness prior for soft decoding of JPEG images," *IEEE Transactions on Image Processing*, vol. 26, no. 2, pp. 509–524, 2017.

[21] P. A. Chou, E. Pavez, R. L. de Queiroz, and A. Ortega, "Dynamic polygon clouds: Representation and compression for VR/AR," Microsoft Research Technical Report, Tech. Rep., 2017.